

Investigations in Abrasive Water Jet Erosion Based on Wear Particle Analysis

A. W. Momber

H. Kwak

R. Kovacevic

Center for Robotics and Manufacturing Systems, University of Kentucky, Lexington, KY

In the study, gray cast iron specimens are cut by abrasive water jets with pressures between $p = 140$ MPa and $p = 345$ MPa. Wear particles collected during cutting are analyzed based on average grain size and grain size distribution. The average diameter of the removed wear particles was found to be between $D = 60 \mu\text{m}$ and $D = 70 \mu\text{m}$ and drops with rising pump pressure. A semi-empirical model is developed to describe this relation. The grain distribution of the wear particles can be characterized by a Rosin-Rammler-Sperling (RRSB)-distribution. The surface area of the removed wear particle samples increases with an increase in the pump pressure. The progress drops at higher pressure levels indicating accelerated efficiency losses if the pump pressure exceeds a certain value. An efficiency parameter, Φ , is defined which relates the jet kinetic energy to the creation of the wear particles, and a method for its estimation is developed. It was found that the efficiency parameter exhibits a maximum value at a pressure level of about three times the material threshold pressure. The average efficiency parameter is estimated to $\Phi = 0.02$.

Introduction

As a new manufacturing process, abrasive water jet (AWJ)-cutting has been very effective for difficult-to-machine materials. From the point of view of jet generation, abrasive water jets can be categorized as injection jets or suspension jets. Injection jets are the most commonly used type for practical applications. An injection AWJ is formed by accelerating small abrasive particles through contact with a high velocity plain water jet. The velocity of the plain water jet can be estimated by applying Bernoulli's law of pressure constancy (Momber, 1993),

$$w_0 = \varphi \cdot \sqrt{\frac{2 \cdot p}{\rho_w}} \quad (1)$$

The mixing between abrasives, water and air takes place in a mixing chamber, whereas the acceleration process occurs in an acceleration tube, or abrasive waterjet nozzle. The abrasive particles leave this nozzle at velocities of several hundred meters per second. The abrasive particle velocity can be approximated by assuming a simple momentum balance in the mixing chamber. Neglecting the mass flow rate of the air which is sucked with the material, the abrasive particle velocity is,

$$w_p = \mu \cdot \frac{w_0}{1 + \frac{\dot{m}_p}{\dot{m}_w}} \quad (2)$$

In Eqs. (1) and (2), the parameters φ and μ are momentum transfer coefficients which can be estimated by jet impact force measurements as outlined by Momber and Kovacevic (1995).

The most pronounced characteristic of AWJ generated surfaces is the presence of striation marks which transpire below a region of relative smooth surface finish. The source of this phenomenon is not clear yet.

Based on observations in transparent materials, Hashish (1988) and Blickwedel (1990) suggest a two-stage cutting process, which consists of a cutting wear stage at small impact

angles and a deformation wear stage at large impact angles. In contrast, Arola and Ramulu (1993) found that the material removal mechanisms are independent on cutting parameters and do not change with the kerf depth. They introduced the idea that striations are results of abrasive energy losses during the cutting process. Chao and Geskin (1993) concluded from surface topography measurements, that the main sources of striation formations are vibrations generated by the cutting machine and that the striation generation is independent on the removal process.

All references used information from the cutting front and the cutting surface to develop their conclusions. No attention is given to the analysis of the wear particles of removed material. It can be assumed that these wear particles contain a high amount of information about the mechanisms involved in their formation. Typical parameters of the particles are their size, size distribution, shape, and structural conditions. Using these parameters the erosion process can be analyzed from the energy point of view (Momber, 1992a, 1993, Momber and Kovacevic, 1994). Also, results from wear particle measurements can be used to analyze the material behavior during erosion (Momber, 1992, 1992b).

Because of the difficulties involved in collecting, separating and treating wear particles during or after the erosion process, the research in this field is limited. Investigations in dry particle erosion of metals, which is very similar to the problem of abrasive water jet erosion, were carried out by Kleis and Uemois (1974), Ruff (1978), Kosel et al. (1984), and Tscherny et al. (1988). Their results are summarized in Table 1. In the field of plain water jet cutting, Fowell and Martin (1993), Momber (1992, 1992a, 1992b, 1993) and Momber and Kovacevic (1994) have done investigations on the wear particles of rocks and concretes. The results of their findings are also listed in Table 1.

The subject of this paper is the investigation of wear particles generated during abrasive water jet erosion of gray cast iron under a given set of process parameters. The philosophy behind this investigation is that size and size distribution of the wear particles may give information about the general mechanism, the energy absorption, and the efficiency of the material removal mechanisms involved in the AWJ cutting process.

Experimental Work

Figure 1 shows the flow chart of the experimental work which was done during the investigation. For cutting the specimens,

Contributed by the Tribology Division for publication in the JOURNAL OF TRIBOLOGY. Manuscript received by the Tribology Division August 15, 1995; revised manuscript received February 22, 1996. Associate Technical Editor: F. E. Kennedy, Jr.

Table 1 Review about wear particle investigations in solid particle erosion and plain water jet cutting

Reference	Problem	Results
Kleis and Uemois (1974)	solid particle erosion of metals	—wear particle shape is irregular —mass ratio wear particle/abrasive particle = 0.1
Ruff (1984)	solid particle erosion of steel	—Contact numbers between 0.1 and 0.25 —erosion mechanism involves removal of plastically deformed material from the lips of impact craters
Kosel et al. (1988)	solid particle erosion of nickel and steel	—erosion debris sizes are between 1 μm and 9 μm —lamellae wear particle shape suggests micromachining at low impact angles
Tscherny et al. (1988)	solid particle erosion of steel	—wide range of particle diameters —constant average wear particle diameter for different erosion conditions
Fowell and Martin (1993)	water jet assisted coal cutting	—contact numbers between 0.1 and 1 —wear particle diameter depends on the brittleness of the target material
Momber and Kovacevic (1994)	plain water jet concrete cutting	—optimum pressure range exists for crack growth through the material —calculation of energy losses due to secondary fragmentation

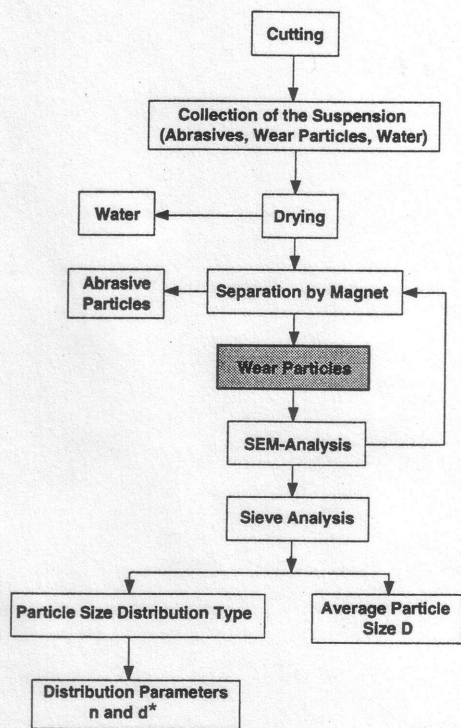


Fig. 1 Flow chart of the experimental work

an abrasive water jet system was used as shown in Fig. 2. The system consists of a double acting high pressure intensifier pump, an AWJ cutting head, an abrasive storage and metering system, a catcher tank, and a x-y-z positioning cutting table controlled by a CNC-controller. As an abrasive material a garnet Mesh #36 was used as shown in Fig. 3. The grain size distribution of the abrasive material is given in Table 2. The average abrasive particle size is $d_A = 485 \mu\text{m}$. The hardness of the abrasive material is about 8 in the Mohs scale, the density is $\rho_p = 4,100 \text{ kg/m}^3$. All cutting parameters and cutting conditions

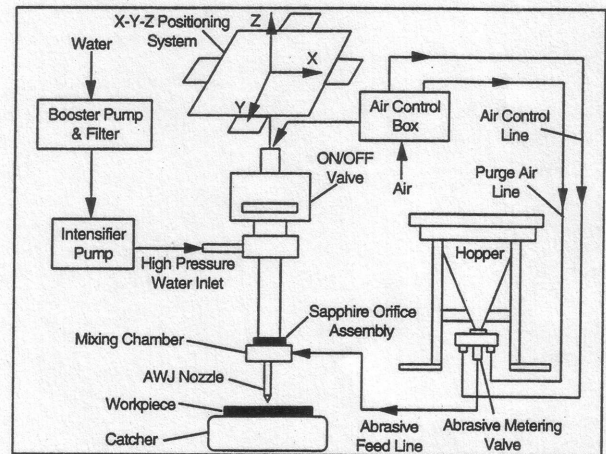


Fig. 2 Structure of the abrasive waterjet cutting system

Nomenclature

c_M = target material sound wave velocity
 D = average wear particle diameter
 d_A = abrasive particle diameter
 d_p = wear particle diameter
 d_w = water jet orifice diameter
 d^* = particle size distribution size modulus
 E = Young's modulus
 E_A = AWJ kinetic energy
 E_C = threshold kinetic energy
 E_{SP} = specific erosion energy
 h = depth of cut
 K_{ic} = target material fracture toughness

L_K = cut length
 M_i = wear particle mass fraction
 \dot{m}_A = abrasive mass flow rate
 \dot{m}_W = water mass flow rate
 n = particle size distribution regularity number
 O = sieve overflow
 p = pump pressure
 p_c = threshold pump pressure
 P_C = mean contact pressure
 p_{OPT} = optimum pump pressure
 S_p = wear particle sample surface
 v = traverse rate

w_p = abrasive particle velocity
 w_0 = water jet velocity
 α = energy transfer coefficient
 χ = energy dissipation coefficient
 $\dot{\epsilon}$ = strain rate
 φ = momentum transfer coefficient orifice
 Φ = efficiency parameter
 Γ = work of fracture
 μ = momentum transfer coefficient mixing chamber
 ρ_M = target material density
 ρ_p = abrasive material density
 ρ_w = water density

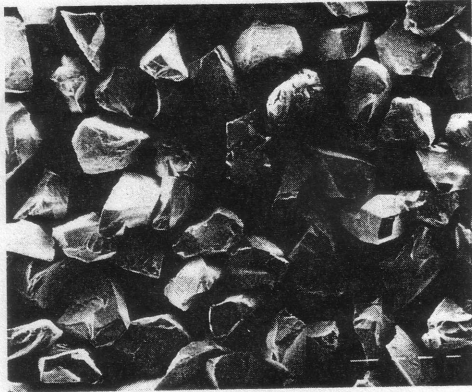


Fig. 3 SEM image of the used abrasive material, scale: 100 μm

are listed in Table 3. The ratio between abrasive mass flow rate and water mass flow rate was between $R = 0.1$ and $R = 0.14$.

The investigated material was a gray cast iron sample, ASTM grade 40. Selected mechanical properties of the material are listed in Table 4. The dimensions of the used specimen are 305 mm in length, 105 mm in width, and 50 mm in height. To consider possible deviations in the workpiece structure as well as in the abrasive water jet formation process, three cuts were generated under each certain parameter combination at different locations of the specimen. The collected three material samples were then unified and analyzed as described in the next subsection to obtain average target parameters. No comparison was made between the three different samples.

A specially designed Plexiglas chamber was used for catching and collecting the suspension consisting of used abrasive particles, process water, and removed wear particles (Fig. 4). The cutting duration was 18 sec for each sample. During this time, about 1.5 g of target material was collected in the chamber. After cutting, suspension was removed from the chamber and dried at room temperature. After drying, the cast iron particles and the abrasive grains were separated by using a magnet. This process was controlled by periodic inspections by SEM and EDS-measurements.

In order to estimate the grain distributions of the collected wear particle samples, *sieve analyses* were carried out. The sieve series was subdivided into five size intervals. The individual sieve sizes were selected following Kelly and Spottiswood (1982). The sieve series as well as the results of the sieve analyses are listed in Table 5. The particle movement during sieving was performed by a commercial sieve shaker.

Experimental Results and Discussion

Average Wear Particle Size. There are several substantial methods to estimate the average diameter of a known particle size distribution (McCabe et al., 1993). Problems related to the characterization of wear debris by an equivalent particle diameter were recently discussed by Heshmat and Brew (1994). It was shown by Guo et al. (1992) for fine grained mineral materi-

Table 3 Cutting conditions and process parameters

Parameter	Definition	Values
Pump pressure	p [MPa]	138 ~ 345
Traverse rate	v [mm/s]	4.2
Standoff distance	s [mm]	9.0
Abrasive flow rate	\dot{m}_A [g/s]	4.3
Abrasive type	—	Garnet
Abrasive size	Mesh	# 36
Impact angle	δ [degree]	90
Orifice diameter	d_w [mm]	0.33
Focus diameter	d_F [mm]	1.02
Focus length	l_F [mm]	76.2

als that the mass related mean diameter gives the most realistic results. The average wear particle diameter, D , is therefore estimated by,

$$D = \frac{\sum_{i=1}^N (d_{p,i} \cdot M_i)}{\sum_{i=1}^N M_i} \quad (3)$$

Here, M_i is the mass fraction of the given particle diameter $d_{p,i}$. The average wear particle diameters calculated from Eq. (3) are plotted against the pump pressure in Fig. 5. The estimated diameter values for the different pump pressure levels are in a narrow range between $D = 60 \mu\text{m}$ and $D = 70 \mu\text{m}$. This narrow range may lead to the assumption that the general removal mechanism does not depend significantly on the applied pump pressure. The same conclusion was made by Arola and Ramulu (1993). Based on SEM observations of aluminum and graphite-epoxy composites, these authors found that the mechanisms of material removal do not change with cutting parameters and depth of cut.

Nevertheless, it can be seen that the average wear particle diameter drops with an increase in the pump pressure. This result from the sieve analysis is supported by SEM-photographs. Figure 6 may serve as an example. The removed cast iron particles are significantly larger at the lower pressure level.

It is of general interest to explain the relation between average wear particle diameter and applied pump pressure, $D = f(p)$, analytically. Derivation for the estimation of the debris size after dynamic fragmentation of brittle solids as presented by Grady (1982) and Glenn et al. (1986) can serve as a base, which is related to the present problem. Based on an energy balance in the fractured material Glenn et al. (1986) obtained,

$$D = \left[\frac{5 \cdot K_{Ic}}{\rho_M \cdot c_M \cdot \dot{\epsilon}} \right]^{2/3} = A_1 \cdot \dot{\epsilon}^{-2/3} \quad (4)$$

The strain rate, $\dot{\epsilon}$, as the only kinematic parameter in Eq. (4), is inversely proportional to the debris size. A method for calculating the strain rate during microparticle impact is given by Hutchings (1977), who found that the order of magnitude of the mean strain rate does not depend on whether plastic flow occurs during impact. In Eq. (5), Hutchings' (1977) formula

Table 2 Grain size distribution of the garnet abrasive particles (Barton Mines Corp., New York)

Sieve diameter (μm)	Mass fraction (%)
300	0.2
355	2.7
425	18.1
500	38.0
600	37.1
710	4.0

Table 4 Material properties of the used gray cast iron

Material property	Value
Density ρ_M	7,200 kg/m ³
Young's modulus E_M	130 GPa
Tensile strength σ_T	260 MPa
Poisson's ratio ¹⁾ ν_M	0.27
Brinell hardness ²⁾ HB	260
Fracture toughness ¹⁾ K_{Ic}	35 MN/m ^{3/2}

¹⁾ From Waterman and Ashby (1991).

²⁾ From Lych (1984).

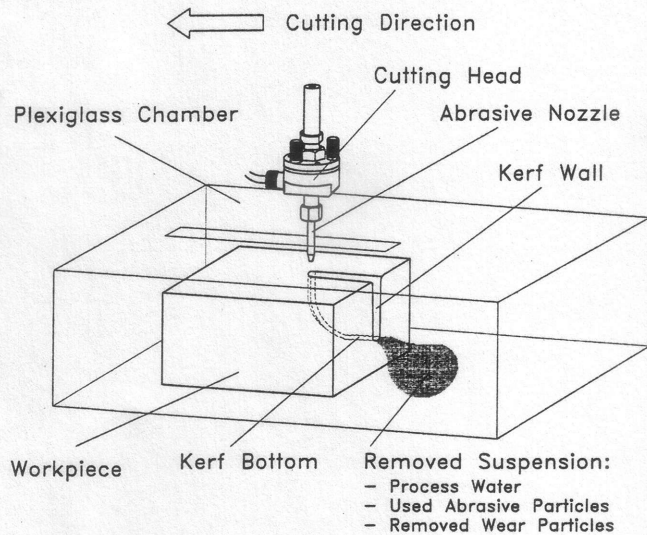


Fig. 4 Design of the suspension collecting unit

for the stress rate is written as a function of the abrasive particle velocity,

$$\dot{\epsilon} = \frac{0.36 \cdot w_p^{1/2}}{d_A} \cdot \left[\frac{1.5 \cdot P_C}{\rho_p} \right]^{1/4} \quad (5)$$

Here, the maximum mean contact pressure, P_C , also depends on the particle impact velocity. It can be calculated by using the Hertzian elastic contact model (Hutchings, 1977),

$$P_C = \left[0.054 \cdot \rho_M \cdot w_p^2 \cdot \left(\frac{1}{f(E)} \right)^4 \right]^{1/5} = A_2 \cdot w_p^{2/5} \quad (6)$$

Applying Bernoulli's law of pressure constancy to the driving water jet and assuming a simple momentum transfer between water jet and abrasive grains, one obtains $w_p = A_3 \cdot p^{1/2}$ (see Eqs. (1) and (2)). If all material parameters in Eqs. (1) to (2) and (4) to (6) are summarized in a constant, the final relation between average wear particle diameter and pump pressure is,

$$D(p) = A_4 \cdot p^{-1/5} \quad (7)$$

The results of Eq. (7) are plotted in Fig. 5. The maximum deviation between analysis and experiment is about 4.5% (correlation 0.93). Therefore, Grady's (1982) and Glenn's et al. (1986) analyses are at least in qualitative agreement with the general trend of the experimental results obtained in this study. The constant A_4 in Eq. (7) includes material parameters from the specimen as well as from the abrasives. The accuracy of Eq. (7) could be improved if A_4 is considered to be a pressure dependent parameter. This modification may take into account

Table 5 Erosion debris sieve analysis results for different pump pressures

Sieve size (μm)	Cumulative sieve passing (%)			
	138 MPa	207 MPa	276 MPa	345 MPa
38	5.4	10.5	12.4	15.1
53	16.2	30.5	31.6	26.8
106	62.1	68.6	69.3	67.0
212	99.5	93.4	96.7	98.5
300	100.0	100.0	100.0	100.0

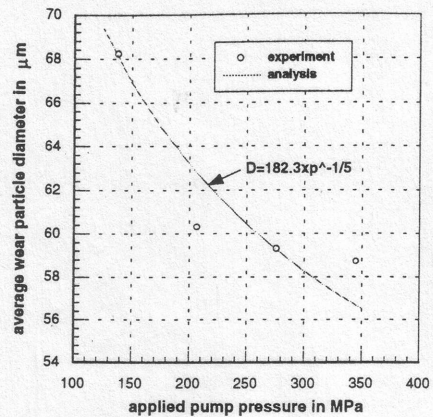
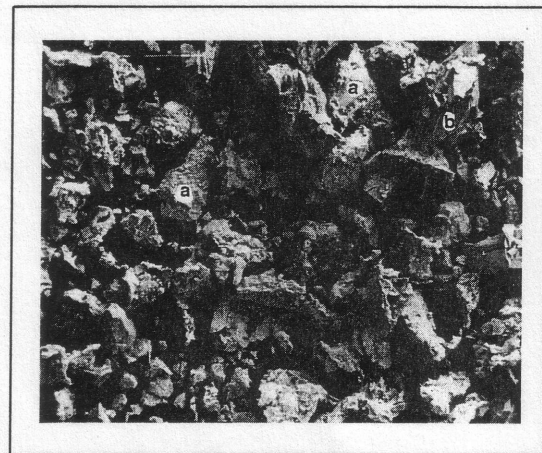


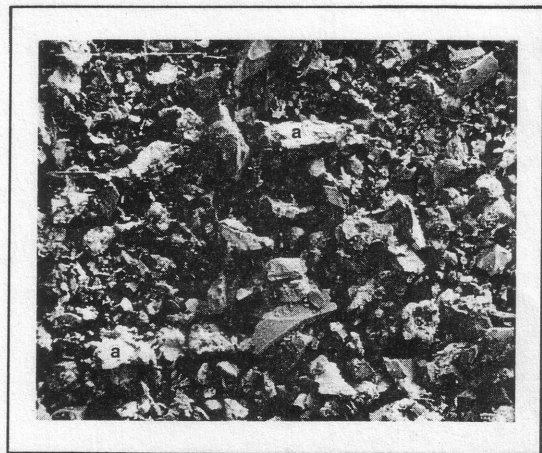
Fig. 5 Relation between applied pump pressure, p , and average wear particle diameter, D

the fact, that some materials properties, such as Young's modulus and fracture toughness, are sensitive to the loading rate.

Wear Particle Size Distribution. A number of equations have been developed to determine the size distribution of comminution products. Reviews are given by Kelly and Spottiswood (1982) and by Schubert (1988). These equations are all of the generalized form,



pump pressure $p=69$ MPa



pump pressure $p=276$ MPa

Fig. 6 SEM images of gray cast iron wear particles (a) and of broken abrasive particles (b); scales: 100 μm

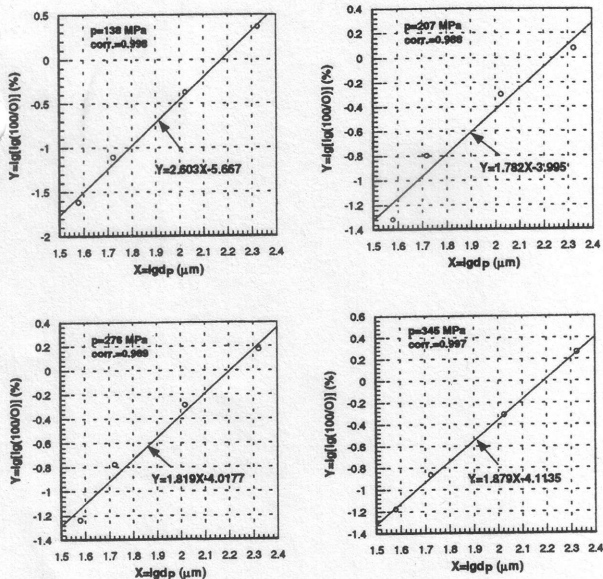


Fig. 7 Characteristics of the Rosin-Rammler-Sperling (RRSB)-distribution for the measured gray cast iron wear particle size distributions, Eq. (11)

$$O = f\left(\frac{d_p}{d^*}\right)^n \quad (8)$$

Here, the parameter d^* is frequently referred to as the size modulus. The exponent n is called the distribution modulus since it is a measure of the spread of the particle sizes in the distribution. Based on the sieve analyses presented in Table 5, it was found that a RRSB-distribution according to Rosin and Rammler (1933) is suitable to describe the distribution of the wear particle sizes in the present study. The same result was obtained by Momber (1992b) for concrete debris after cutting by plain water jets. The RRSB-distribution is usually written as,

$$O = 100 \cdot \exp\left[\left(-\frac{d_p}{d^*}\right)^n\right] \quad (9)$$

Equation (9) can be rewritten as,

$$\frac{100}{O} = \exp\left[\left(\frac{d_p}{d^*}\right)^n\right] \quad (10)$$

After logarithmizing Eq. (10) twice one obtains a linear relation,

$$\underbrace{\lg\left[\lg\left(\frac{100}{O}\right)\right]}_Y = \underbrace{n \cdot \lg d_p}_A + \underbrace{C_1}_B \quad (11)$$

Here, $A = n$, and $B = \lg(\lg e) - n \cdot d^*$.

A comparison between Eq. (11) and the results of the sieve analyses is presented in Fig. 7. The regression coefficients of the linear regressions are larger than $R^2 = 0.98$ indicating that Eq. (11) is fulfilled. In the special case of a RRSB-distribution, the size modulus, d^* , is a characteristic grain diameter for $O = 36.8\%$ and, under some limitations, can describe the fineness of the grain sample. It is not identical to the average wear particle diameter, D . The size modulus can be calculated by,

$$d^* = 10^{(\lg[\lg(100/36.2)] - C_1)/n} \quad (12)$$

The estimated values are between $d^* = 99 \mu\text{m}$ and $d^* =$

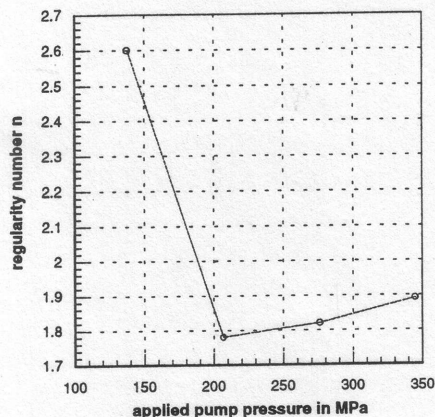


Fig. 8 Relation between applied pump pressure, p , and regularity number of the Rosin-Rammler-Sperling (RRSB)-distribution, n

110 μm , they show the same pump pressure dependence as the average wear particle diameters calculated from Eq. (3).

The RRSB-distribution parameter n can be assumed as a regularity number. For conventional mechanical comminution processes this parameter ranges from $n = 0.7$ to $n = 1.4$ (Schubert, 1988). In the range $n > 1$ it can be used to describe the homogeneity of the grain size distribution. The value for n is infinite if the grain sample consists of grains with identical diameters. Related to the present problem this would be valid in an idealized homogeneous material removal process. Therefore, the regularity number can characterize the machining regime. The parameter n can easily be estimated from Eq. (11) to $n = A = \Delta Y / \Delta X$. The results of these calculations are presented in Fig. 8. As Fig. 8 shows, the values of n depend on the pump pressure. They lie between $n = 1.9$ and $n = 2.6$ and exhibit a minimum in a pump pressure range of $p = 200$ MPa. These values are remarkably higher than regularity numbers reported for mechanical fragmentation processes, and also slightly higher than regularity numbers obtained during concrete removal by plain water jets which are reported by Momber (1992b). This suggests that abrasive water jet erosion is a comparably controlled destruction process. The cuts in glass specimens which are shown in Fig. 9, confirm this conclusion. The kerf structure is extremely unsteady in the case of plain water jet cutting without abrasive particles. In contrast, the kerfs generated by abrasive water jets have a defined shape and a regular structure.

As in the case of the average wear particle diameter, the narrow range of the values of the regularity number suggests that the general material removal mechanism does not depend on the applied pressure.

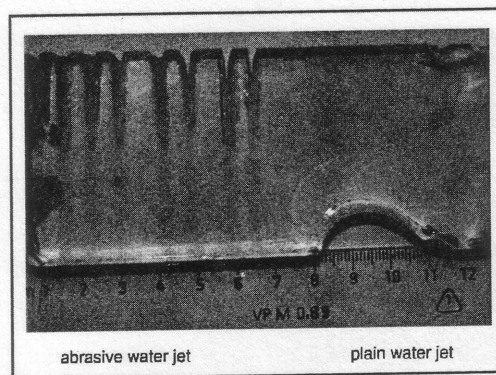


Fig. 9 Kerf structures in a glass sample subjected by a plain water jet (right part) and an abrasive water jet (left part); applied pump pressure: $p = 100$ MPa

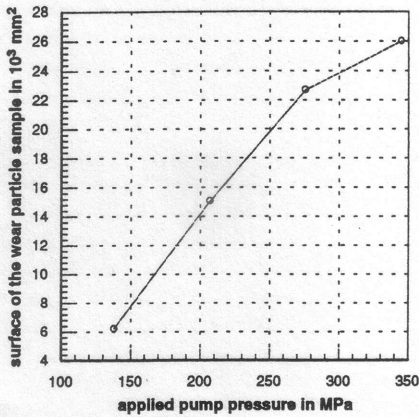


Fig. 10 Relation between applied pump pressure, p , and generated surface of the wear particle samples, S_p , calculated from Eq. (13)

Surface of the Wear Particle Samples. As shown in the previous chapter, the wear particle grain size distributions can be represented by a RRSB-distribution. This fact enables the direct estimation of the surface of the investigated grain collections, S_p , by using the distribution parameters d^* and n . Assuming spherical wear particles, the surface of the RRSB-distributed particle sample is (Schubert, 1988),

$$S_p = V_p \cdot \frac{6 \cdot n}{(d^*)^n} \cdot \int_{d_U}^{d_O} d_p^{n-2} \cdot \exp\left[\left(-\frac{d_p}{d^*}\right)^n\right] d d_p, \quad (13)$$

with $d_U = d_p(O = 99.9\%)$, and $d_O = d_p(O = 0.1\%)$. The integral in Eq. (13) can be solved by a series expansion. In Fig. 10, the estimated surface values are plotted against the pump pressure. The surface increases with rising pressure which can be explained by the smaller average particle diameter and the higher fineness of the debris samples, and of course by the larger number of removed grains, for higher pressures. Interestingly, the function drops at a pump pressure range of $p = 300$ MPa. This fact is in agreement with results from the kerf depth measurements and the target material volume loss measurements in the present study (see Fig. 11).

This latter observation is a significant sign of efficiency losses. In the reference literature, the drop in the efficiency of AWJ in the range of high pressures is explained by decreased mixing and acceleration efficiency (Hashish, 1989). But there should be some additional effects that are related to the material

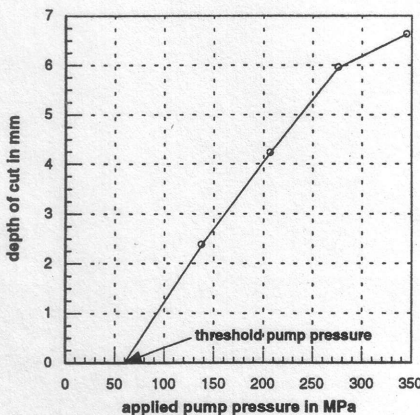


Fig. 11 Relation between applied pump pressure, p , and generated depth of cut, h

removal process. A possible way to treat this problem is discussed in the next chapter.

Definition and Estimation of an Efficiency Number

Based on an energy balance (Momber and Kovacevic, 1994a) it can be shown that the energy which is dissipated by the material during the machining with AWJ is,

$$E_{ab} = \chi(h) \cdot [E_A - E_C] \quad (14)$$

For the condition in this study (blind kerfing), $\chi(h) = 1$ (Momber and Kovacevic, 1994a). The relation between AWJ kinetic energy and pump pressure is,

$$E_A = \frac{1.11 \cdot \alpha \cdot d_w^2 \cdot L_K}{\sqrt{\rho_w \cdot \nu}} \cdot p^{3/2} = \psi \cdot p^{3/2}. \quad (15)$$

According to Uetz and Khosrawi (1980), the energy of an impacting abrasive particle is dissipated by the specimen due to elastic work, E_{el} , plastic work, E_{pl} , the generation of new surfaces, E_O , and heat, E_{th} . An energy balance gives,

$$\psi \cdot [p^{3/2} - p_C^{3/2}] = E_{el} + E_{pl} + E_O + E_{th}. \quad (16)$$

The ratio between the right term and the left term of Eq. (16) yields an efficiency value Φ . For simplifying the procedure, the energy terms E_{el} and E_{th} in Eq. (16) are excluded. According to the classical energy balance of fracture mechanics (Lawn and Wilshaw, 1975), the energy required for creating new surfaces for an idealized brittle fracture is proportional to the materials specific surface energy. Results from Rao and Buckley (1985) show that the specific surface energy can be related to the solid particle erosion process in metals. Uetz and Khosrawi (1980) related the volume removal from particle erosion directly to the specific surface energy. Soemantri and Finnie (1985) successfully applied a modified specific energy parameter, which lies between the thermodynamic specific surface energy and the specific work of fracture, to describe the solid particle erosion of copper. A similar approach was used by Zeng and Kim (1992) who used the specific surface energy for modeling the removal of ceramics by AWJs. In the present study, the presence of plastic deformation is observed (Fig. 6). The fact that plastic work contributes to the fracture of materials is considered in the models of Orowan and Irwin (see Lawn and Wilshaw, 1975). The energy for the generation of new surfaces is then a summary of different energy portions which are summarized in a parameter Γ , often called the work of fracture. Using these assumptions the energy which is absorbed during the generation of the wear particles is approximately,

$$E_{pl} + E_O \approx 2 \cdot \Gamma \cdot S_p. \quad (17)$$

Using Eqs. (3) to (17), the efficiency parameter can be calculated,

$$\Phi = \frac{2 \cdot \Gamma \cdot S_p \cdot \sqrt{\rho_w \cdot \nu}}{1.11 \cdot \alpha \cdot d_w^2 \cdot L_K \cdot p^{3/2}} \quad (18)$$

Equation (18) is applied to estimate the relation between pump pressure and efficiency as plotted in Fig. 12. For the work of fracture a value of $\Gamma = 4,500$ J/m² is used for the cast iron (Waterman and Ashby, 1991).

The efficiency values are between $\Phi = 0.017$ and $\Phi = 0.024$ which means that about 2% of the AWJ input energy is absorbed due to the generation of the surfaces of the wear particles. This value is in the range of mechanical crushing processes where efficiency values between $\Phi = 0.001$ and $\Phi = 0.02$ are reported (McCabe et al. 1993), and also in the range of abrasion processes which have an efficiency of about $\Phi = 0.01$ (Ruff, 1978).

In Fig. 12, the results of Eq. (18) are approximated by a 4th-order polynomial regression. The regression function shows that the efficiency of the material removal process exhibits a maxi-

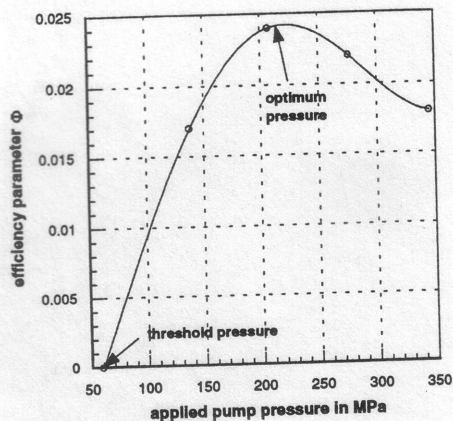


Fig. 12 Relation between applied pump pressure, p , and efficiency parameter Φ , calculated from Eq. (18)

imum at a pump pressure of about $p_{OPT} = 210$ MPa. From Fig. 11, one can derive an almost linear relation between the pump pressure and the depth of cut,

$$h(p) = C_2 \cdot (p - p_c). \quad (19)$$

The threshold pressure, p_c , describes the minimum pump pressure required for material removal process. This threshold pressure is simply the crossing point between the pressure axis and the function $h(p)$. In the present case, $p_c = 62$ MPa (see Fig. 11). According to Eq. (15) the relation between the energy of an AWJ and the pump pressure is $E_A = \psi \cdot p^{3/2}$. Therefore, the specific erosion energy can be written,

$$E_{SP} = \frac{E_A}{h} = \frac{\psi \cdot p^{3/2}}{C_2 \cdot (p - p_c)}. \quad (20)$$

For an effective removal process, E_{SP} should be minimized. Thus, the first deviation of Eq. (20) must become zero, $dE_A/dh = 0$. It can be shown, that the solution of this criteria is,

$$p_{OPT} = 3 \cdot p_c \quad (21)$$

For the given threshold pressure in this study, Eq. (21) delivers an optimum pump pressure of $p_{OPT} = 186$ MPa which is in good agreement with the optimum pump pressure obtained from Fig. 12.

Summary

The results of the investigation can be summarized as follows:

—Wear particles of gray cast iron collected during AWJ cutting at pump pressures between $p = 138$ MPa and $p = 345$ MPa are analyzed based on the average grain size and grain size distribution.

—For the given process conditions the average diameter of the removed wear particles lies between $D = 60 \mu\text{m}$ and $D = 70 \mu\text{m}$ and drops with rising pump pressure. A semi-empirical model is developed to describe this relation.

—The grain distribution of the wear particles, $O(d_p)$, can be characterized by a Rosin-Rammler-Sperling (RRSB)-distribution. The regularity number of this distribution, n , increases slightly with the applied pump pressure in high pump pressure ranges.

—The surface of the removed wear particle samples, S_p , linearly increases with the pump pressure at lower pressure ranges. The function drops at higher pressure ranges indicating accelerated efficiency losses if the pressure exceeds a certain limit.

—An efficiency parameter, Φ , is defined and a method for its estimation is developed. It is found that about 2% of the AWJ input energy is absorbed due to the generation of the wear particles. The efficiency parameter shows a maximum at a pump pressure of $p_{OPT} = 3 p_c$.

—It is concluded that the primary material removal mechanism does not depend significantly on the pump pressure applied in this study, but it is found that the pump pressure influences the efficiency of the material removal process.

Acknowledgments

The authors are thankful to the Center for Robotics and Manufacturing Systems at the University of Kentucky, Lexington, and to the Alexander-von-Humboldt Foundation, Bonn, Germany, for their financial support.

References

- Arola, D., and Ramulu, M., 1993, "Mechanisms of Material Removal in Abrasive Waterjet Machining of Common Aerospace Materials," *Proceedings, 7th American Water Jet Conference*, M. Hashish, ed., Water Jet Techn. Association, St. Louis, Vol. 1, pp. 43–64.
- Blickwedel, H., 1990, "Erzeugung und Wirkung von Hochdruck-Abrasivstrahlen," Ph.D. thesis, Hannover University, Hannover.
- Chao, J., and Geskin, E., 1993, "Experimental Study of the Striation Formation and Spectral Analysis of the Abrasive Waterjet Generated Surfaces," *Proceedings, 7th American Water Jet Conference*, M. Hashish, ed., Water Jet Techn. Association, St. Louis, Vol. 1, pp. 27–41.
- Fowell, R. J., and Martin, J. A., 1993, "Water Jet Assisted Coal and Rock Cutting," *Geomechanics*, 93, Z. Rakowski, ed., Balkema, Rotterdam, pp. 247–254.
- Grady, D. E., 1982, "Local Effects in Dynamic Fragmentation," *Journal of Applied Physics*, Vol. 53, pp. 322–325.
- Guo, N. S., Louis, H., Meier, G., and Ohlsen, J., 1992, "Recycling Capacity of Abrasives in Abrasive Water Jet Cutting," *Jet Cutting Technology*, A. Lichtarowicz, ed., Kluwer Acad. Publ., Dordrecht, pp. 503–523.
- Hashish, M., 1988, "Visualization of the Abrasive Waterjet Cutting Process," *Experimental Mechanics*, Vol. 24, pp. 159–169.
- Hashish, M., 1989, "Pressure Effects in Abrasive-Waterjet (AWJ) Machining," *ASME Journal of Engineering Materials and Technology*, Vol. 111, pp. 221–228.
- Heshmat, H., Brewe, D. E., 1994, "On the Cognitive Approach Toward Classification of Dry Triboparticles," *20th Leeds-Lyon Symposium of Dissipative Processes in Tribology*, Elsevier Tribology Series, Elsevier Sci. Pub., London.
- Hutchings, I. M., 1977, "Strain Rate Effects in Microparticle Impact," *Journal of Physics, D: Applied Physics*, Vol. 10, pp. L179–L184.
- Kelly, E. G., Spottiswood, D. J., 1982, "Introduction to Mineral Processing," John Wiley & Sons, New York.
- Kleis, J., Uemois, U., 1974, "Untersuchungen zum Strahlverschleibmechanismus von Metallen," *Zeitschrift für Werkstofftechnik*, Vol. 5, pp. 381–389.
- Kosel, T. H., Mao, Z. Y., and Prasad, S. V., 1984, "Erosion Debris Particle Observation and the Micromachining Mechanisms of Erosion," *ASLE Transactions*, Vol. 28, pp. 268–276.
- Lawn, B. R., Wilshaw, T. R., 1975, *Fracture of Brittle Solids*, Cambridge University Press, Cambridge.
- Lynch, C. T., 1984, *CRC Handbook of Materials Science*, Vol. II, CRC Press, Boca Raton.
- Momber, A., 1992, "Investigations on Water Jet Processed Concrete," *Jet Cutting Technology*, A. Lichtarowicz, ed., Kluwer Acad. Publ., Dordrecht, pp. 405–412.
- Momber, A., 1992a, "Energetical Aspects of Mass Concrete Removal Using Plain High Speed Water Jets," *Decommissioning and Demolition*, I. L. White, ed., Thomas Telford Ltd, London, pp. 95–101.
- Momber, A., 1992b, "Untersuchungen zum Verhalten von Beton unter der Belastung durch Druckwasserstrahlen," *VDI-Fortschrittsberichte*, Reihe 4, No. 109, VDI-Verlag, Düsseldorf, pp. 1–137.
- Momber, A., 1993, "Ein zerkleinerungstechnischer Aspekt der Betonbearbeitung mittels Druckwasserstrahlen," *Aufbereitungstechnik*, Vol. 34, pp. 252–256.
- Momber, A., 1993b, "Handbuch Druckwasserstrahl-Technik," Beton Verlag GmbH, Düsseldorf.
- Momber, A., Kovacevic, R., 1994, "Secondary Fragmentation in Water Jet Cutting of Brittle Multiphase Material," *Jet Cutting Technology*, N. G. Allen, ed., Mech. Eng. Publ., London, pp. 139–150.
- Momber, A., Kovacevic, R., 1994a, "Calculation of Exit Jet Energy in Abrasive Water Jet Cutting," *PED-Vol. 68-1*, pp. 361–366.
- Momber, A., Kovacevic, R., 1995, "Energy Dissipative Processes in High Speed Water-Solid Particle Erosion," *HTD-Vol. 231/FED-Vol. 233*, pp. 243–256.
- Rao, P. V., Buckley, D. H., 1985, "Characterization of Solid Particle Erosion

Resistance of Ductile Materials Based on their Properties," *ASME Journal of Engineering for Gas Turbines and Power*, Vol. 107, pp. 669-678.

Rosin, P., Rammler, E., 1933, "The Laws Governing the Fineness of Powdered Coal," *Journal Inst. Fuel*, Vol. 7, pp. 29-36.

Ruff, A. W., 1978, "Debris Analysis of Erosive and Abrasive Wear," *Fundamentals of Tribology*, N. P. Shuh and N. Saka, eds., MIT Press, Cambridge, pp. 877-885.

Schubert, H., 1988, "Aufbereitung fester mineralischer Rohstoffe," VEB Deutscher Verlag für Grundstoffindustrie, Leipzig, Vol. 1, pp. 31-34.

Soemantri, S., Finnie, I., 1985, "The Size Effect in Abrasion, Erosion, Grinding and Cutting of Metals," *PED-Vol. 16*, pp. 35-44.

Tscherny, S., Wandtke, E., and Fröhner, U., 1988, "Beitrag zur Klärung von Strahlverschleiß-Vorgängen auf der Grundlage von Partikeluntersuchungen," *Schmierungstechnik*, Vol. 19, pp. 235-239.

Uetz, H., Khosrawi, M. A., 1980, "Strahlverschleiß," *Aufbereitungstechnik*, No. 5, pp. 253-266.

Waterman, N. A., Ashby, M. F., 1991, *CRS-Elsevier Materials Selector*, Vol. 2, CRS Press, Boca Raton.

Zeng, J., Kim, T. J., 1992, "Development of an Abrasive Waterjet Kerf Cutting Model for Brittle Materials," *Jet Cutting Technology*, A. Lichtarowicz, ed., Kluwer Acad. Publ., Dordrecht, pp. 483-501.

Papers and Publications of Special Interest to Tribologists

Journal of Applied Mechanics, Vol. 63, September 1996

Z. S. Olesiak and Yu. A. Pyryev, "Transient Response in a One-Dimensional Model of Thermoelastic Contact," p. 575.

Z. S. Olesial and Yu. A. Pyryev, "On Nonuniqueness and Stability in Barber's Model of Thermoelastic Contact," p. 582.

E. S. Edelstein and J. J. Blech, "Rotation of a Clamped Spherical Ball Due to Linear Reciprocating Motion," p. 683.

Journal of Engineering Materials and Technology, Vol. 118, July 1996

Hyo-Sok Ahn et al., "Nondestructive Detection of Damage Produced by a Sharp Indenter in Ceramics," p. 402.